Flat-topped optical spectrum as a specific marker of multi-pulse grouping in soliton fiber laser

DMITRY KOROBKO,[1,*] VALERIA RIBENEK,[1] PAVEL ITRIN[1] AND ANDREI FOTIADI[1,2]

[1]*Ulyanovsk State University, 42 Leo Tolstoy Street, Ulyanovsk, 432017, Russia*
[2]*University of Mons, 7000 Mons, Belgium*
**korobkotam@rambler.ru*

Received XX Month XXXX; revised XX Month, XXXX; accepted XX Month XXXX; posted XX Month XXXX (Doc. ID XXXXX); published XX Month XXXX

We report the experimental observation of a stable generation regime in a soliton fiber laser, characterized by a distinct flat-topped optical spectrum. Notably, in multi-pulse generation, this specific spectrum shape prevents the harmonic mode-locking state, instead connecting the solitons into bound complexes or tight chaotic bunches. Physically, this suggests that in the observed regime, long-range attractive forces dominate over inter-pulse repulsion across the entire laser cavity. Our experimental findings align with numerical simulations, which demonstrate that the predominance of long-range inter-pulse attraction is due to a complex interaction mechanism. This mechanism combines the generation of dispersive waves with dissipative forces arising from gain depletion and recovery.

Passively mode-locked fiber lasers have potential applications in creating compact, robust, and stable ultra-short pulse sources. Multiple pulse generation is a common feature of mode-locked fiber lasers with anomalous dispersion, exploiting soliton propagation. Various multi-soliton ensembles can be developed by balancing different interacting forces acting on solitons within a fiber cavity [1-3]. These multi-soliton formations exhibit diverse dynamics, ranging from weakly interacting soliton gas to bound pulse states with fixed spacing, known as "soliton molecules," and pulse bunches where the solitons chaotically move within a narrow cavity area [2-4].

Generally, the interactions governing the formation of these multi-pulse patterns can be either repulsive or attractive. Predominance of long-range repulsive forces leads to an evenly spaced cavity distribution of pulses, also known as harmonic mode-locking (HML) [5]. Specifically, methods that increase the intensity of inter-pulse repulsion have been shown to improve HML stability, which is crucial for many applications [6, 7]. The balance between long-range attractive and repulsive forces is a typical feature of "loosely bound" solitons with time separations of hundreds to thousands of pulse durations [2, 8]. Conversely, the prevalence of attraction leads to the development of compact chaotic soliton bunches or soliton bound states with fixed inter-pulse time distances within the group [1-3, 8-10]. Experimental determination of soliton complex types and their dynamics is performed through the investigation of oscilloscope traces and pulse group autocorrelations. Observations of the laser optical spectrum can provide additional information about the phase relationships between pulses [10, 11].

There is a great deal of variety in the nature of attractive and repulsive interactions in soliton fiber lasers. The primary long-range interaction mechanisms include those mediated by gain depletion and recovery (GDR) [12], guided acoustic wave Brillouin scattering [13, 14], and interactions transmitted through dispersive waves (DW) or continuous wave (CW) backgrounds co-propagating with the pulses in the laser cavity (DW-interaction) [6, 15]. One of the key challenges in fiber laser physics is to uncover and explain the interaction mechanism governing the observed pulse group dynamics. Some approaches to solve this problem involve real-time ultrafast measurements, which aim to unveil more direct information about interaction intensities and the dynamics of processes under their influence [3, 5, 16]. This work demonstrates that considerable information about the nature of forces acting on solitons can be obtained from the shape of the laser's optical spectrum. By varying the polarization settings of a fiber laser mode-locked through nonlinear polarization evolution (NPE), we discovered a stable generation regime with a specific flat-topped shape of the optical spectrum. This shape is distinct from the typical soliton spectrum and slightly resembles the spectrum of dissipative solitons in fiber lasers with normal dispersion. Interestingly, this regime completely excludes HML during multi-pulse generation, and in its entire region of existence, only the formation of various compact pulse groups is observed. Our conclusions align with several experimental observations of soliton bound states and bunches with a similar optical spectrum shape [17-19]. These results suggest that the flat-topped spectrum of a mode-locked fiber laser can serve as an indicator of the dominance of long-range mutual attractive forces acting on the scale of the whole cavity.

The experimental configuration of an Er-doped soliton nonlinear polarization evolution (NPE) mode-locked fiber ring laser is shown in Fig. 1. The unidirectional laser cavity consists of two types of fibers: a 0.8 m length of heavily erbium-doped fiber (EDF) with normal dispersion (-48 ps/nm /km) and a standard single mode fiber (G.652.D, Fujikura) with anomalous dispersion (17 ps/nm/km). The fiber isolator (ISO) and in-line polarizer supplied by PM output fibers (~0.5 m), two 980/1550 WDM couplers, 3-

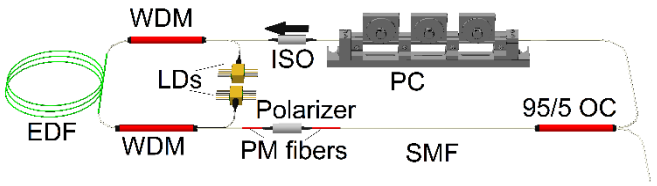

Fig.1. Fig. 1. Experimental setup of the soliton NPE-mode-locked laser. EDF: Erbium-doped fiber; WDM: wavelength division multiplexer; LDs: pump laser diodes; SMF: single-mode optical fiber; PM fibers: polarization-maintaining optical fibers; ISO: optical fiber isolator; OC: optical coupler; PC: polarization controller.

paddle fiber polarization controller (PC) and 5% output coupler (OC) constitute the ring laser cavity with the ~15m total length and fundamental laser frequency of $f_0 = 13.43$ MHz . The central wavelength of the soliton laser can be tuned simply by adjusting PC that controls a linear birefringence filter formed in the cavity fiber. The laser could be tuned to the wavelengths selected from bands between 1550 and 1590 *nm* specific for the built fiber configuration. The laser operation is monitored using an optical spectrum analyzer (Yokogawa 6370D) with a resolution of ~0.02 *nm*, a radiofrequency spectrum analyzer (R&S FSP40) and a ~ 4 *GHz* digital oscilloscope (Keysight) both coupled with a 30 *GHz* photodetector.

By adjusting the polarization controller properly, at pump power equal to ~ 100 *mW* we observe the stable single pulse generation at fundamental frequency with typical flat-topped spectrum and widened Kelly sidebands (Fig. 2). Output power of laser at single pulse generation is equal to ~ 0.13 *mW* corresponding to output soliton energy ~ 10 *pJ*. The obtained autocorrelation trace can be referred to in inset showing the pulse width is ~ 0.49 *ps* assuming a sech^2 pulse profile. The TBP is calculated to be ~ 0.55 corresponding to slightly chirped soliton.

As the pump power increases, the laser switches to multi-pulse generation. In this regime, the laser's radiofrequency spectrum maintains its structure with a period equal to the fundamental frequency f_0, while autocorrelation traces show that the number of pulses increases proportionally with the pump power (Fig. 3(a)). This indicates that all pulses in the cavity are clustered in a single bound state. The optical spectrum of this bound state retains its flat-topped shape with widened sidebands and exhibits a typical fringe structure with a period inversely proportional to the inter-pulse distance (Fig. 3(b)). Careful adjustment of the PC, while maintaining the optical spectrum shape, can vary the number of solitons in the bound state or result in a compact chaotic soliton bunch. Additionally, adjusting the PC can transform the existing soliton bound state into a periodic pulse distribution of harmonic mode-locking (HML), though this significantly alters the optical spectrum shape. For comparison, the optical spectrum of the laser in the HML state is also shown in Fig. 2.

The experimental results allow us to draw the following conclusions. The discovered generation regime of a standard soliton fiber laser, characterized by a wide (>9 *nm*) flat-topped spectrum, widened sidebands and ultrashort sub-picosecond soliton duration during multi-pulse generation, corresponds to the suppression of large-scale mutual pulse repulsion, leading to the formation of compact soliton complexes. To elucidate the nature of the inter-pulse interaction, we performed a series of numerical simulations based on the fiber laser configuration. The numerical model of the NPE mode-locked fiber ring laser, similar to those

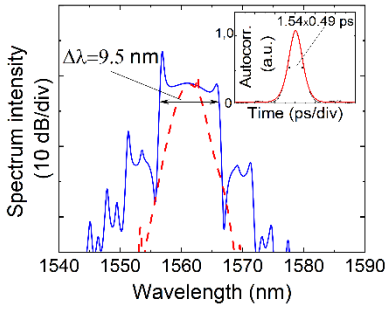

Fig. 2. Optical spectrum and autocorrelation (inset) of the laser in the single-pulse generation mode. The dashed line shows the optical spectrum of the laser in the HML state with a pulse repetition rate of 0.72 GHz. In the latter case, the pump power is ~160 mW.

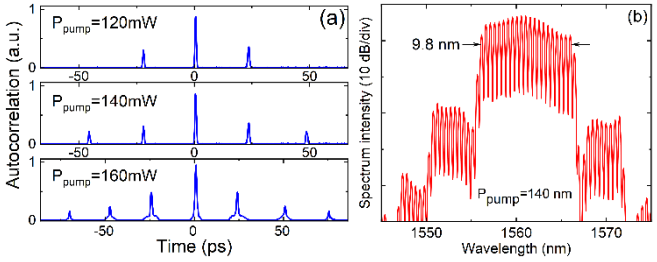

Fig. 3. (a) Autocorrelations of bound soliton states observed at different pump levels. From top to bottom: two, three, and four bound solitons. (b) Optical spectrum of bound soliton states.

Table 1. The system parameters used in simulations

Parameter	Value	Parameter	Value
λ_0 (nm)	1560	$\Omega_g/2\pi$ (THz)	8 (~ 65 nm in the range near $\lambda_0 = 1560$ nm)
β_2 (ps^{2}m^{-1})	-0.02	l_g (m)	0.8
β_{2g} (ps^{2}m^{-1})	0.045	l_{SMF} (m)	14.2
$\gamma = \gamma_g$ (W^{-1} m^{-1})	0.002	g_0 (m^{-1})	3
ρ	0.85	E_g (pJ)	$k \cdot 92.5$

referenced in [6, 20], utilizes parameter values close to our experimental configuration (Table 1), where l_g and l_{SMF} are the lengths, β_{2g} and β_2 are the group velocity dispersions (GVD), γ_g and γ are the Kerr nonlinearities of the gain fiber and passive SMF, respectively. The gain spectral filtering is centered at the wavelength λ_0 and employed using a parabolic approximation with the FWHM gain line bandwidth Ω_g ; g_0 and E_g are the small signal gain and gain saturation energy, respectively. All linear losses within the cavity are accounted for as local losses in the output coupler, described by its power transmission coefficient ρ^2 : $A' = \rho A$. Periodic boundary conditions with a window size of $\tau_{win} = 2^{13} \cdot 0.02\text{ps} \cdot k$ (where k is the number of simulated pulses in the cavity) consisting of $2^{13} \cdot k$ points are used for simulation. In this context, τ_{win} can be considered as the fundamental period of the

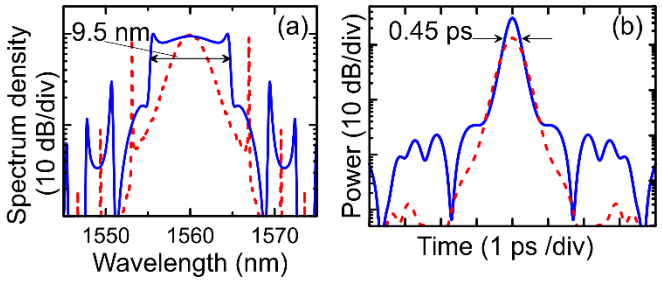

Fig. 4. Results of numerical simulations. (a) Spectrum and (b) log-scaled pulse envelop obtained for the single pulse generation with the next polarizer and PC settings: $\theta = 0.6, \Delta\varphi = 3\pi/5, \varphi = 2.25$. Dashed lines correspond to the single pulse obtained for alternate settings: $\theta = 0.7, \Delta\varphi = \pi/2, \varphi = 2.1$. In multi-pulse generation with incorporated time-dependent gain, the alternate settings correspond to the HML state.

laser cavity. The control parameters of the model are the orientations of the PC and polarizer: θ , φ and phase difference introduced by the PC: $\Delta\varphi$.

Correct selection of these control parameters ensures the successful implementation of NPE mode-locking, where initial low-amplitude Gaussian noise is converted into ultrashort soliton pulses within a few tens of cavity roundtrips. Fig. 4 shows the results of numerical simulations for single pulse generation with the following parameter settings: $\theta = 0.6, \Delta\varphi = 3\pi/5, \varphi = 2.25$. The simulated spectrum shape and pulse duration are quite close to the experimental results. Notably, the generated ultrashort soliton possesses a powerful dispersive pedestal. We believe that the specific spectrum shape with widened Kelly sidebands observed both experimentally and in simulations (Fig. 4(a)) results directly from highly efficient four-wave mixing (FWM) between the soliton and its dispersive pedestal.

To explain the group soliton dynamics in multi-pulse generation, we need to introduce inter-pulse interaction into the numerical model through the addition of time-dependent gain $g_{TD}(t)$, which is a small parameter compared to the spectrally limited time-independent saturated gain g . The time dependence of $g_{TD}(t)$ originates from the depletion and recovery of ion population inversion in the gain medium and can be determined by the standard rate equation:

$$\frac{dg_{TD}}{dt} = \frac{g_{TD0} - g_{TD}}{\tau_g} - \frac{g_{TD}|A(t)|^2}{E_g} \qquad \textbf{(1)}$$

where τ_g is the relaxation time of the gain medium and $|A(t)|^2$ is the signal power. It is well known [12] that due to the tendency of a single pulse to achieve a higher level of instantaneous gain g_{TD} , a dissipative force of mutual repulsion appears in the ring fiber cavity. Thus, in the absence of other inter-pulse interactions, the gain depletion and recovery (GDR) effect leads to the emergence of the HML laser state. Recently, it has been shown [20] that the generation of dispersive waves (DW) significantly influences the GDR soliton interaction process. Specifically, the time-dependent gain asymmetry induces phase asymmetry in the soliton dispersive pedestal and shifts the resonant DW frequencies. If the nonlinear FWM process between the soliton and DWs is highly efficient, the asymmetry of instantaneous gain leads to energy redistribution between the spectral soliton components, resulting in soliton drift to the region of lower gain. This means that the GDR mechanism can facilitate not only soliton repulsion but also a previously unexplored phenomenon of GDR+DW-induced soliton attraction. Through numerical simulations of soliton interactions within the fiber cavity, we have discovered that the flat-topped shape of the optical spectrum with typical widened Kelly sidebands can be considered a distinctive marker of this process, demonstrating high intensity of FWM between the soliton and its dispersive pedestal. All these conclusions are confirmed by numerical simulations of the model with parameters corresponding to our experimental setup, including an additionally introduced small time-dependent gain with relaxation time $\tau_g = 0.5\mu s \gg T_R$.

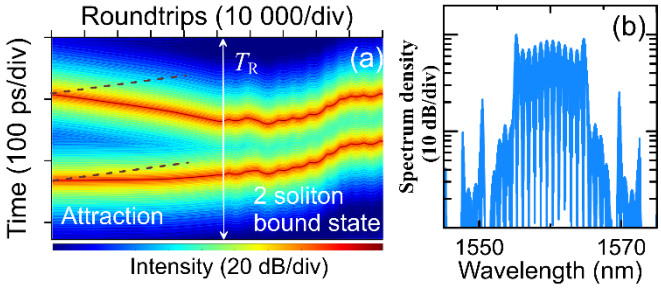

Fig. 5. Results of numerical simulations. (a) Evolution of a soliton pair in the fiber laser cavity with specific polarizer and PC settings $\theta = 0.6, \Delta\varphi = 3\pi/5, \varphi = 2.25$ (same as in Fig. 4(a, b) - solid lines). Dashed lines show the pulse trajectories without the incorporation of time-dependent gain. (b) Spectrum of the 2-soliton bound state formed during the evolution of the initial soliton pair.

Fig. 5(a) shows the results of numerical simulations of our laser with initial conditions corresponding to a soliton pair exhibiting a typical flat-topped spectrum (polarization settings are the same as in Fig. 4). For comparison, the dashed lines in Fig. 5(a) represent the soliton trajectories when the effect of time-dependent gain $g_{TD}(t)$ is completely "turned off." In this case, the solitons interact only through direct DW-interaction, and the straight-line trajectories with constant inter-pulse time distance indicate negligible intensity of this interaction. Conversely, the introduction of time-dependent gain induces noticeable changes in the soliton trajectories, shifting them to the right from the undistorted paths to regions of lower time-dependent gain due to the cooperative action of GDR and DW [20]. As a result, the solitons experience an attractive force that draws them closer. After tens of thousands of cavity roundtrips, the distance between the solitons decreases, and the force of direct DW-interaction increases. As the solitons gradually approach each other, the attractive GDR + DW forces and the repulsive forces induced by the direct DW-interaction eventually, balance out. This results in two solitons co-propagating with an approximately constant inter-pulse time distance, equating to hundreds of soliton durations, thereby forming a loosely bound soliton state. Ultimately, after the formation of the bound state, the soliton drift velocities align, and the solitons form a joint spectrum with interference fringes typical of a bound state (Fig. 5(b)). Importantly, the optical spectrum shape of the soliton bound state closely resembles the optical spectrum shape of a single soliton with the same control parameters. Maintaining this specific spectrum shape indicates the continuation

of efficient FWM between the soliton and DWs during the interaction.

The approach of introducing small time-dependent gain to describe soliton interaction is versatile. Similar to the experiment, the control parameters of the numerical model can be adjusted such that the initial pulse pair evolves into the HML state with a periodic pulse distribution, where the inter-pulse distance is equal to $T_R/2$. This transition in control settings $\theta = 0.7, \Delta\varphi = \pi/2, \varphi = 2.1$ also leads to significant changes in the spectrum shape and output pulse parameters (Fig. 4 - dashed lines). The optical spectrum shape now resembles a typical soliton spectrum with narrow resonant Kelly sidebands, and the pulse envelope exhibits lower peak power, longer time duration, and a weaker dispersive pedestal. We propose that this reduction in pedestal power is responsible for the decreased FWM efficiency and the transformation of GDR + DW soliton attraction into pure GDR-induced repulsion.

In conclusion, our experiments demonstrate that the mode-locking state of a soliton fiber laser with a specific flat-topped optical spectrum and widened Kelly sidebands exhibits distinctive and intriguing properties. We found that in multi-pulse generation, this specific spectrum shape completely eliminates the harmonic mode-locking state, instead grouping the solitons into bound complexes or tight chaotic bunches. Physically, this indicates that this spectrum shape corresponds to the predominance of long-range attractive forces over inter-pulse repulsion across the entire laser cavity. The harmonic mode-locking (HML) laser state becomes possible only after tuning the polarization settings, which alters the spectrum form and restores the ability for long-range repulsion.

Our experimental results align with our simulation findings, which show that the emergence of prevailing long-range inter-pulse attraction can be explained by the combined effects of gain depletion and recovery along with the generation of powerful dispersive waves (DWs). An important component of this complex attractive mechanism is the effective four-wave mixing (FWM) between the soliton and DWs, which is responsible for developing the peculiar flat-topped spectrum shape. Numerical simulations performed with parameter values close to our experimental setup confirmed these conclusions.

Funding. Russian Science Foundation (#23-79-30017).

Disclosures. The authors declare no conflicts of interest.

Data availability. Data underlying the results presented in this paper may be obtained from the authors upon reasonable request.

References

1. Z. Q. Wang, K. Nithyanandan, A. Coillet, *et al.*, Nature communications **10**, 830 (2019).
2. D. A. Korobko, R. Gumenyuk, I. O. Zolotovskii, *et al.*, OFT **20**, 593 (2014).
3. J. Peng and H. Zeng, Laser & Photonics Reviews **12**, 1800009 (2018).
4. F. Amrani, A. Haboucha, M. Salhi, *et al.,* Applied Physics. B **99**, 107 (2009).
5. X. Liu and M. Pang, Laser & Photonics Reviews **13**(9), (2019).
6. D. A. Korobko, V. A. Ribenek, D. A. Stoliarov, *et al.*, Optics Express **30**, 17243 (2022).
7. D. A. Korobko, V. A. Ribenek, P. A. Itrin, *et al.*, Optics & Laser Technology **162**, 109284 (2023).
8. T. Zhu, Z. Wang, D. N. Wang, *et al.*, Photonics Research **7**, 61 (2018).
9. L. M. Zhao, D. Y. Tang, H. Zhang, *et al.*, Optics Express **17**, 8103 (2009).
10. A. Haboucha, H. Leblond, M. Salhi, *et al.,* Physical Review. A **78**, (2008).
11. L. Gui, X. Xiao, and C. Yang, JOSA B **30**, 158 (2012).
12. J. N. Kutz, B. C. Collings, K. Bergman, *et al.*, " IEEE Journal of Quantum Electronics **34**, 1749 (1998).
13. A. N. Pilipetskii, E. A. Golovchenko, and C. R. Menyuk, Optics Letters **20**, 907 (1995).
14. V. A. Ribenek, P. A. Itrin, D. A. Korobko, *et al.*, APL Photonics **9**, (2024).
15. D. Y. Tang, B. Zhao, L. M. Zhao, *et al.,* Physical Review. E **72**(1), (2005).
16. J. Zeng and M. Y. Sander, Optics Letters **45**, 5 (2019).
17. D. D. Han and L. Yun, Laser Physics **22**(12), 1837 (2012).
18. H. Haris, T. S. Jin, M. Batumalay, *et al.,* Nanomaterials **13**(9), 1538 (2023).
19. Z. Wang, Z. Wang, Y. Liu, *et al.*, Chinese Optics Letters **15**(8), 080605 (2017).
20. D. A. Korobko, V. A. Ribenek, and A. A. Fotiadi, Journal of Lightwave Technology 1–9 (2024).

References

1. Wang, Z. Q., Nithyanandan, K., Coillet, A., Tchofo-Dinda, P., & Grelu, P. (2019). Optical soliton molecular complexes in a passively mode-locked fibre laser. Nature communications, 10(1), 830.
2. D. A. Korobko, R. Gumenyuk, I. O. Zolotovskii, and O. G. Okhotnikov, “Multisoliton complexes in fiber lasers,” Optical Fiber Technology, vol. 20, no. 6, pp. 593–609, (2014).
3. J. Peng and H. Zeng, "Build‐Up of dissipative optical soliton molecules via diverse soliton interactions," Laser & Photonics Reviews 12(8), 1800009 (2018).
4. F. Amrani, A. Haboucha, M. Salhi, H. Leblond, A. Komarov, and F. Sanchez, "Dissipative solitons compounds in a fiber laser. Analogy with the states of the matter," Applied Physics. B, Lasers and Optics 99(1–2), 107–114 (2009).
5. X. Liu and M. Pang, "Revealing the buildup dynamics of harmonic Mode‐Locking states in ultrafast lasers," Laser & Photonics Reviews 13(9), (2019)
6. D. A. Korobko, V. A. Ribenek, D. A. Stoliarov, P. Mégret, and A. A. Fotiadi, "Resonantly induced mitigation of supermode noise in a harmonically mode-locked fiber laser: revealing the underlying mechanisms," Optics Express 30(10), 17243 (2022).
7. D. A. Korobko, V. A. Ribenek, P. A. Itrin, D. A. Stoliarov, and A. A. Fotiadi, "Polarization maintaining harmonically mode-locked fiber laser with suppressed supermode noise due to continuous wave injection," Optics & Laser Technology/Optics and Laser Technology 162, 109284 (2023).
8. T. Zhu, Z. Wang, D. N. Wang, F. Yang, and L. Li, "Observation of controllable tightly and loosely bound solitons with an all-fiber saturable absorber," Photonics Research 7(1), 61 (2018).
9. L. M. Zhao, D. Y. Tang, H. Zhang, and X. Wu, "Bunch of restless vector solitons in a fiber laser with SESAM," Optics Express 17(10), 8103 (2009).
10. A. Haboucha, H. Leblond, M. Salhi, A. Komarov, and F. Sanchez, "Analysis of soliton pattern formation in passively mode-locked fiber lasers," Physical Review. A 78(4), (2008).
11. L. Gui, X. Xiao, and C. Yang, "Observation of various bound solitons in a carbon-nanotube-based erbium fiber laser," Journal of the Optical Society of America. B, 30(1), 158 (2012).
12. J. N. Kutz, B. C. Collings, K. Bergman, et al., "Stabilized pulse spacing in soliton lasers due to gain depletion and recovery," IEEE Journal of Quantum Electronics 34, 1749 (1998).
13. A. N. Pilipetskii, E. A. Golovchenko, and C. R. Menyuk, "Acoustic effect in passively mode-locked fiber ring lasers," Optics Letters/Optics Index 20(8), 907 (1995).
14. V. A. Ribenek, P. A. Itrin, D. A. Korobko, and A. A. Fotiadi, "Double harmonic mode-locking in soliton fiber ring laser acquired through the resonant optoacoustic coupling," APL Photonics 9(5), (2024).
15. D. Y. Tang, B. Zhao, L. M. Zhao, and H. Y. Tam, "Soliton interaction in a fiber ring laser," Physical Review. E 72(1), (2005).
16. J. Zeng and M. Y. Sander, "Real-time transition dynamics between multi-pulsing states in a mode-locked fiber laser," Optics Letters 45(1), 5 (2019).
17. D. D. Han and L. Yun, "Observations of three types of sidebands in a passively mode-locked soliton fiber laser," Laser Physics **22**(12), 1837–1841 (2012).
18. H. Haris, T. S. Jin, M. Batumalay, A. R. Muhammad, J. Sampe, A. M. Markom, H. A. Zain, S. W. Harun, M. M. I. M. Hasnan, and I. Saad, "Single and bunch soliton generation in optical fiber lasers using bismuth selenide topological insulator saturable absorber," Nanomaterials 13(9), 1538 (2023).
19. Z. Wang, Z. Wang, Y. Liu, R. He, G. Wang, G. Yang, and S. Han, "Generation and time jitter of the loose soliton bunch in a passively mode-locked fiber laser," Chinese Optics Letters 15(8), 080605 (2017).
20. D. A. Korobko, V. A. Ribenek, and A. A. Fotiadi, "Gain depletion and recovery as a key mechanism of Long-Range pulse interactions in soliton fiber laser," Journal of Lightwave Technology 1–9 (2024).